Organic & Biomolecular Chemistry

Cite this: *Org. Biomol. Chem.*, 2012, **10**, 8434

www.rsc.org/obc

PAPER

Experimental and theoretical study of the [3 + 2] cycloaddition of carbonyl ylides with alkynes†

Ghenia Bentabed-Ababsa,*[a,b] Samira Hamza-Reguig,[a] Aïcha Derdour,[a] Luis R. Domingo,*[c] José A. Sáez,[c] Thierry Roisnel,[d] Vincent Dorcet,[d] Ekhlass Nassar[e] and Florence Mongin*[b]

Received 24th July 2012, Accepted 11th September 2012
DOI: 10.1039/c2ob26442k

The [3 + 2] cycloaddition reaction between carbonyl ylides generated from epoxides and alkynes (phenylacetylene, methyl propiolate, methyl but-2-ynoate and methyl 3-phenylpropiolate) to give substituted 2,5-dihydrofurans was investigated. The effect of indium(III) chloride on the outcome of the reaction was studied in the case of phenylacetylene and methyl propiolate. The thermal reaction between the carbonyl ylide coming from 2,2-dicyano-3-phenyloxirane and both methyl propiolate and methyl but-2-ynoate was theoretically investigated using DFT methods in order to explain the reactivity and regioselectivity observed.

Introduction

Cycloaddition reactions are one of the most important synthetic processes, with both synthetic and mechanistic interest in organic chemistry. Among them, [3 + 2] cycloaddition (32CA) reactions, also named 1,3-dipolar cycloadditions, whose general concept was introduced by Huisgen and co-workers in 1960s,[1] are versatile tools for building five-membered heterocycles, and current understanding of the underlying principles in these reactions has grown from a fruitful interplay between theory and experiment.[2]

Carbonyl ylides, generated by thermal ring opening of epoxides, are known to react with π-bonds of alkynes,[3] alkenes,[3a,b,4] imines,[5] aldehydes[5c,6] and ketones,[7] and thioketones,[8] affording highly substituted dihydrofurans, tetrahydrofurans, oxazolidines, dioxolanes, and oxathiolanes, respectively. Following recent studies of the 32CA reactions between, on the one hand, carbonyl ylides and, on the other hand, aldehydes,[5c] imines,[5c] and ketones,[7] in which we have performed theoretical calculations using density functional theory (DFT) methods to depict the mechanism of these reactions, we here report our studies concerning the reactions involving unsymmetrical alkynes.

Since the first thermal reactions between carbonyl ylides, generated from epoxides, and activated alkynes (such as methyl acetylenedicarboxylate) reported more than 40 years ago,[3a,b] few studies have been devoted to such an access to dihydrofurans.[3c–e] In particular, it was of interest to study, in the light of DFT calculations, the regioselectivity results obtained by involving unsymmetrical alkynes in the reaction with carbonyl ylides.

Results and discussion

Synthetic aspects

We first considered 32CA reactions between 2,2-dicyano-3-(4-substituted)phenyloxiranes **1a–c**[9] and terminal alkynes. Using phenylacetylene (**2**, 5 equiv.), monitoring the conversion to the corresponding 2,5-dihydrofurans by TLC showed that the reactions carried out in refluxing toluene were complete after about 40 h. NMR analysis of the crude obtained after removal of the solvent showed the presence of two regioisomers in each case,

[a]*Laboratoire de Synthèse Organique Appliquée, Faculté des Sciences, Université d'Oran, BP 1524 El M'Naouer, 31000 Oran, Algeria. E-mail: badri_sofi@yahoo.fr; Fax: +213-04158-2540; Tel: +213-79175-8768*
[b]*Equipe Chimie et Photonique Moléculaires, Institut des Sciences Chimiques de Rennes, UMR 6226 CNRS, Université de Rennes 1, Bâtiment 10A, Case 1003, Campus Scientifique de Beaulieu, 35042 Rennes Cedex, France. E-mail: florence.mongin@univ-rennes1.fr; Fax: +33-2-2323-6955; Tel: +33-2-2323-6931*
[c]*Departamento de Química Orgánica, Universidad de Valencia, Dr. Moliner 50, 46100 Burjassot, Valencia, Spain. E-mail: domingo@utopia.uv.es; Fax: +34-9-6354-4328; Tel: +34-9-6354-3106*
[d]*Centre de Diffractométrie X, Institut des Sciences Chimiques de Rennes, UMR 6226 CNRS, Université de Rennes 1, Bâtiment 10B, Campus Scientifique de Beaulieu, 35042 Rennes Cedex, France*
[e]*Department of Chemistry, Faculty of Women for Arts, Science and Education, Ain Shams University, Asma Fahmy Street, Heleopolis (El-Margany), Cairo, Egypt*

†Electronic supplementary information (ESI) available: ^{1}H and ^{13}C NMR spectra of the compounds **3a–c**, **3′b**, **5a–c**, **5′a–c**, **8a–c** and **9a–c**; ORTEP diagrams of the compounds **3a–c**, **5′a**, **5b**, **8a** and **8b**. For the stationary points involved in the 32CA reactions of CY **1′a** with methyl propiolate (**4**) and methyl but-2-ynoate (**6**): B3LYP/6-31G*, B3LYP/6-311G* and B3LYP/6-311+G* total and relative energies *in vacuo* and transition state geometries, B3LYP/6-31G* solvent energies and thermodynamic data, and B3LYP/6-31G* cartesian coordinates. CCDC **3a** (891057), **3b** (891058), **3c** (891059), **5′a** (891060), **5b** (891061), **8a** (891062), and **8b** (891063). For ESI and crystallographic data in CIF or other electronic format see DOI: 10.1039/c2ob26442k

Table 1 Cycloaddition reaction between carbonyl ylides generated from the epoxides **1** and phenylacetylene (**2**)

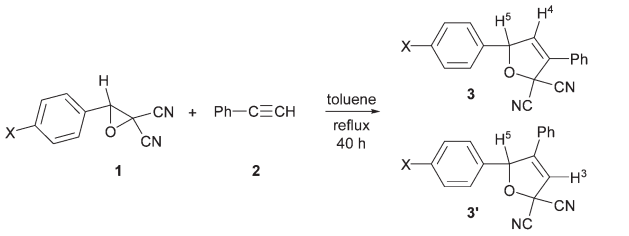

Entry	X (**1**)	Catalyst	**3** : **3′** ratio	Product(s), yield(s) (%)
1	H (**1a**)	—	84 : 16	**3a**, 40
2	Cl (**1b**)	—	84 : 16	**3b**, 52; **3′b**, 12
3	MeO (**1c**)	—	75 : 25	**3c**, 50
4	H (**1a**)	$InCl_3$ (0.1 equiv.)	90 : 10	**3a**, 60
5	Cl (**1b**)	$InCl_3$ (0.1 equiv.)	89 : 11	**3b**, 64
6	MeO (**1c**)	$InCl_3$ (0.1 equiv.)	83 : 17	**3c**, 60

Table 2 Cycloaddition reaction between carbonyl ylides generated from the epoxides **1** and methyl propiolate (**4**)

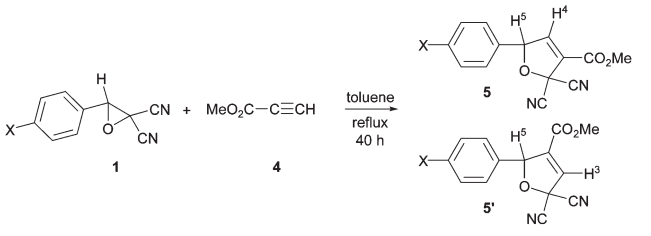

Entry	X (**1**)	Catalyst	**5** : **5′** ratio	Product(s), yield(s) (%)
1	H (**1a**)	—	24 : 76	**5a**, 12; **5′a**, 40
2	Cl (**1b**)	—	26 : 74	**5b**, 10; **5′b**, 54
3	MeO (**1c**)	—	29 : 71	**5c**, 11; **5′c**, 65
4	H (**1a**)	$InCl_3$ (0.1 equiv.)	33 : 67	**5′a**, 58
5	Cl (**1b**)	$InCl_3$ (0.1 equiv.)	31 : 69	**5′b**, 57
6	MeO (**1c**)	$InCl_3$ (0.1 equiv.)	18 : 82	**5c**, 8; **5′c**, 67

with ratios of 84 : 16, 84 : 16 and 75 : 25 respectively obtained using **1a** (X = H), **1b** (X = Cl) and **1c** (X = OMe). The major products **3** were purified by column chromatography over silica gel, in yields ranging from 40 to 52% whereas **3′b** was the only minor product isolated (12% yield). The observed ^{1}H NMR coupling constants of 1.8 and 2.1 Hz were respectively attributed to $^HJ_{4-5}$ (major regioisomer **3**) and $^HJ_{3-5}$ (minor regioisomer **3′**) on the basis of a previous study.[10] The major regioisomers **3** were then identified unequivocally by X-ray structure analysis (Table 1, entries 1–3†).

The same reactions have then been repeated, but in the presence of indium(III) chloride (0.1 equiv.) which has been recognized as a suitable catalyst for cycloaddition reactions.[11] Shortened reaction times of 29 h, 27 h and 20 h increased **3** : **3′** ratios of 90 : 10, 89 : 11 and 83 : 17, and higher yields of **3** (60 to 64%) were respectively noted using **1a** (X = H), **1b** (X = Cl) and **1c** (X = OMe) under these conditions using 4 equiv. of phenylacetylene (Table 1, entries 4–6).

We next turned to the reaction of methyl propiolate (**4**) with the 2,2-dicyano-3-(4-substituted)phenyloxiranes **1a,b** (4 equiv.) and **1c** (1 equiv.) under the conditions used before. Without a catalyst, NMR analysis of the crudes showed the formation of two regioisomers in 24 : 76, 26 : 74 and 29 : 71 ratios, using **1a** (48 h reaction time for complete conversion), **1b** (48 h) and **1c** (24 h) respectively. They were separated by column chromatography over silica gel, and isolated in yields ranging from 10 to 12% and 40 to 65% for the major and minor isomer, respectively. As before,[10] the major compounds with the higher 2,5-dihydrofuran ^{1}H NMR coupling constants (2.1 Hz) were assigned to the 4-substituted regioisomers **5′** ($^HJ_{3-5}$), and the minor compounds with the lower 2,5-dihydrofuran ^{1}H NMR coupling constants (1.5–1.8 Hz) to the 3-substituted regioisomers **5** ($^HJ_{4-5}$). This was corroborated by NMR HMQC sequences performed on **5′c** and **5c**, and the structures of **5′a** and **5b** were confirmed by X-ray diffraction data (Table 2, entries 1–3†). In the presence of indium(III) chloride (0.1 equiv.), the reaction times were slightly shortened (36 h in the case of **1a**,**b** and 20 h with **1c**), as well as the regioselectivities (Table 2, entries 4–6).

Table 3 Cycloaddition reaction between carbonyl ylides generated from the epoxides **1** and methyl but-2-ynoate and 3-phenylpropiolate (**6**,**7**)

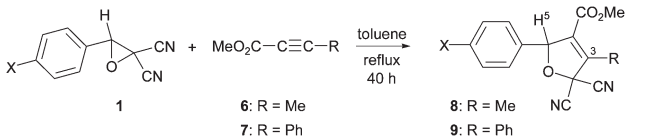

Entry	X (**1**)	R	Reaction time (h)	Product, yield (%)
1	H (**1a**)	Me (**6**)	48	**8a**, 66
2	Cl (**1b**)	Me (**6**)	48	**8b**, 62
3	MeO (**1c**)	Me (**6**)	24	**8c**, 44
4	H (**1a**)	Ph (**7**)	96	**9a**, 60
5	Cl (**1b**)	Ph (**7**)	96	**9b**, 47
6	MeO (**1c**)	Ph (**7**)	55	**9c**, 66

We then considered 32CA reactions between 2,2-dicyano-3-(4-substituted)phenyloxiranes **1a–c** and internal alkynes. Using methyl but-2-ynoate (**6**) and methyl 3-phenylpropiolate (**7**) without catalyst proved completely regioselective. The cycloadducts **8** and **9** respectively formed (extended reaction times were required in the case of **7**) were isolated after purification by column chromatography over silica gel in 44–66% yields (Table 3).

What is remarkable about the ^{1}H NMR spectra of the compounds **8** is a 2.1 Hz coupling constant between the methyl protons (2.44 ppm) and H5 (6.18 ppm) (see Table 3). The presence of a methyl group at C3, already shown on **8c** by an NMR HMQC sequence, was confirmed by X-ray diffraction on crystals of **8a,b**, allowing an unambiguous assignment (Table 3, entries 1–3†).

2,2-Dicyano-3-(4-chlorophenyl)oxirane (**1c**) was also reacted with 3-phenylpropiolonitrile (**10**) as before to afford the expected product **11**. The reaction nevertheless proved less efficient, and the cycloadduct **11** could not be separated from the dioxolanes **12** coming from a reaction with the aldehyde resulting from epoxide degradation (Scheme 1).

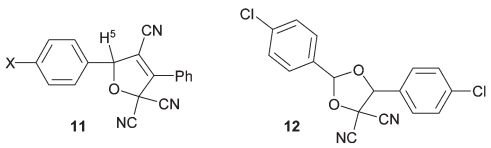

Scheme 1 The different products obtained by the reaction of 2,2-dicyano-3-(4-chlorophenyl)oxirane (**1c**) with 3-phenylpropiolonitrile (**10**).

Calculations

Mechanistic study of the 32CA reactions of the carbonyl ylide 1′a with methyl propiolate (4) and methyl but-2-ynoate (6)

In order to explain the reactivity and regioselectivity of the 32CA reactions of the carbonyl ylide (CY) **1′a** with methyl propiolate (**4**) and methyl but-2-ynoate (**6**), the mechanisms of these cycloaddition reactions were theoretically studied using DFT methods at the B3LYP/6-31G* level.

The CY **1′a** can adopt the *E* or *Z* configuration through the restricted rotation of the C1–O2 bond. In this way, while (*E*)-**1′a** adopts a planar rearrangement, (*Z*)-**1′a** is twisted as a consequence of the hindrance between the phenyl and one cyano group. This hindrance makes (*Z*)-**1′a** 8.6 kcal mol^{-1} higher in energy than (*E*)-**1′a**. In addition, the barrier height associated with the C1–O2 bond rotation is very large, 27.1 kcal mol^{-1}.[5c] Consequently, only the *E* configuration of the CY **1′a** is considered in the present study.

Due to the asymmetry of both reagents, two competitive reaction channels are feasible for each 32CA reaction. They are related to the two regioisomeric approach modes of the CY **1′a** towards the alkynes **4** and **6**, named **m** and **o** (the **m** and **o** acronyms, traditionally used to refer to the relative *meta* and *ortho* positions in the benzene series, are here employed to distinguish the cycloadduct (CA) with distant ester and nitrile functions from that with adjacent ester and nitrile functions). Along the channel **m**, the C1–C5 and C3–C4 bonds are formed, while along the channel **o**, the C1–C4 and C3–C5 bonds are formed. The two regioisomeric channels were studied. Analysis of the stationary points associated with these 32CA reactions indicates that they have a one-step mechanism. Therefore, two transition states (TSs), **TSxm** and **TSxo**, and two CAs, **CAxm** and **CAxo**, were located and characterized for each 32CA reaction (see Scheme 2).

The two 32CA reactions present very low activation barriers: 2.3 kcal mol^{-1} for **TS1m** and 3.6 kcal mol^{-1} for **TS2m** (see Table 4). On the other hand, the two regioisomeric TSs are 2.0

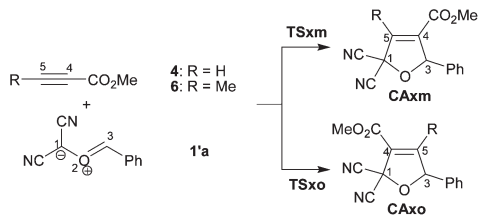

Scheme 2 32CA reactions between CY **1′a** and methyl propiolate (**4**) or methyl but-2-ynoate (**6**).

Table 4 Relative energies (ΔE, in kcal mol^{-1}, relative to **1′a** + **4** and **1′a** + **6**) in gas phase and in toluene, and relative enthalpies (ΔH, in kcal mol^{-1}), entropies (ΔS, in eu) and free energies (ΔG in kcal mol^{-1}) at 110 °C in toluene of the stationary points involved in the 32CA reactions of CY **1′a** with methyl propiolate (**4**) and methyl but-2-ynoate (**6**)

	ΔE	$\Delta E_{toluene}$	ΔH	ΔS	ΔG
TS1m	2.3	4.4	4.7	−42.3	20.9
TS1o	4.3	6.1	6.2	−41.0	21.9
CA1m	−71.9	−68.4	−66.2	−47.0	−48.1
CA1o	−72.6	−69.5	−67.3	−48.3	−48.7
TS2m	3.6	6.3	6.4	−47.1	24.4
TS2o	7.9	9.8	9.8	−44.2	26.8
CA2m	−68.3	−64.4	−62.7	−52.6	−42.5
CA2o	−69.5	−66.1	−64.4	−51.4	−44.6

(**TS1o**) and 4.3 (**TS2o**) kcal mol^{-1} higher in energy than those associated with the most favorable channels **m**. These results agree entirely with the experimentally observed regioselectivity. In this way, a mixture of **CA1m** and **CA1o** is expected for the 32CA reaction between **1′a** and **4**, while for the reaction with **6** only one CA, **CA2m**, is expected. Experimentally, a **CA1m** : **CA1o** 76 : 24 mixture is obtained. All these 32CA reactions are strongly exothermic: between −68.3 and −72.6 kcal mol^{-1}.

The B3LYP/6-31G* geometries were further optimized using the 6-311G* and 6-311+G* basis sets. The energy results are given in the ESI† part. A comparison of the relative energies using the three selected basis sets indicates that there are no significant differences. The activation energies increase slightly with the size of the basis set, but this fact is a consequence of the higher stabilization of CY **1′a** than the TSs. Anyway, the regioselectivity found at these 32CA reactions is kept no matter which basis set is used.

Recent studies devoted to 32CA reactions have shown that solvent effects in the geometry optimization have poor effects due to the low polar character of both TSs and CAs, and of toluene and dichloromethane solvents.[12] Consequently, solvent effects of toluene on energies were considered through single-point energy calculations over the gas-phase optimized geometries using the PCM method. Solvent effects stabilize all species between 2 and 7 kcal mol^{-1} (see Table 4), with the reagents being more stabilized than the TSs.[12] Therefore, the activation barrier for the cycloadditions increases by 2.1 (**TS1m**) and 2.7 (**TS2m**) kcal mol^{-1}. However, solvent effects do not change the gas phase regioselectivity. Therefore, solvent effects appear to have little influence on these 32CA reactions.

Further thermodynamic calculations with regard to toluene showed a similar free energy difference between each pair of regioisomeric TSs (see Table 4). Adding thermal corrections to energies and entropies increases the activation free energies to 20.9 (**TS1m**), 21.9 (**TS1o**), 24.4 (**TS2m**) and 26.8 (**TS2o**) kcal mol^{-1}. Several conclusions can be drawn from these energies: (i) these free activation energies are not very high. However, the endergonic character of the formation of the CY **1′a**, which raises the activation free energies of these 32CA reactions to 29.6 (**TS1m**) and 33.1 (**TS2m**) kcal mol^{-1}, is responsible for the high temperature demanded in these thermal reactions.[7] Note that the free energy of the CY **1′a** is 8.7 kcal mol^{-1} above than the corresponding epoxide;[7] (ii) the presence of an electron-

releasing methyl group in methyl but-2-ynoate (**6**) increases the free activation energy by 3.5 kcal mol^{-1} relative to that using methyl propiolate (**4**); (iii) the regioselectivity measured as the activation free energy difference between the two regioisomeric TSs remains almost unaltered after the thermodynamic calculations: $\Delta G_{(\mathbf{TS1o-TS1m})}$ = 1.0 kcal mol^{-1} and $\Delta G_{(\mathbf{TS2o-TS2m})}$ = 2.4 kcal mol^{-1}; and (iv) these 32CA reactions are strongly exergonic: between −42.5 to −48.7 kcal mol^{-1}. Consequently, these reactions are irreversible.

The B3LYP/6-31G* geometries of the TSs associated with the 32CA reactions between the CY **1′a** and methyl propiolate (**4**) and methyl but-2-ynoate (**6**) are given in Fig. 1, while those obtained using the 6-311G* and 6-311+G* basis sets are given in the ESI† part. At the TSs associated with the 32CA reaction between the CY **1′a** and methyl propiolate (**4**), the lengths of the C–C forming bonds are 2.375 Å (C1–C5) and 2.505 Å (C3–C4) at **TS1m**, and 2.283 Å (C3–C5) and 2.626 Å (C1–C4) at **TS1o**, while those in the 32CA reaction involving methyl but-2-ynoate (**6**) are 2.487 Å (C1–C5) and 2.374 Å (C3–C4) at **TS2m**, and 2.415 Å (C3–C5) and 2.484 Å (C1–C4) at **TS2o**. A comparison of these lengths with those obtained using the 6-311G* and 6-311+G* basis sets indicates that there are no significant geometrical differences.

The electronic structure of the TSs involved in the 32CA reactions between the CY **1′a** and methyl propiolate (**4**) and methyl but-2-ynoate (**6**) was analyzed using the Wiberg bond order[13] (BO) and charge transfer (CT) at the TSs. The extent of bond formation at the TSs is provided by the BOs. At the TSs associated with the 32CA reaction between the CY **1′a** and methyl propiolate (**4**), the BO values of the C–C forming bonds are 0.22 (C1–C5) and 0.17 (C3–C4) at **TS1m**, and 0.26 (C3–C5) and 0.15 (C1–C4) at **TS1o**, while those in the 32CA reaction involving methyl but-2-ynoate (**6**) are 0.22 (C1–C5) and 0.19 (C3–C4) at **TS2m**, and 0.22 (C3–C5) and 0.18 (C1–C4) at **TS2o**. Several conclusions can be drawn from these values: (i) the relative low BO values found at the four TSs indicate that they have an earlier character, in clear agreement with the very low activation energies and the high exothermic character of these processes;[14] (ii) the similar BO values of the two forming bonds at the TSs indicate that they do not present a marked asynchronicity in bond formation as would be expected in a polar process involving asymmetric reagents; (iii) in the four TSs, the C–C bond formation at the β position of **4** and **6** is slightly more advanced than at the α position.

The polar or non-polar character of these 32CA reactions was analyzed evaluating the CT at the four TSs. The natural charges were shared between the CY and the alkyne frameworks. At the TSs, the charge at the CY framework is 0.05 at **TS1m**, 0.02 at **TS1o**, 0.00 at **TS2m** and −0.01 at **TS2o**. These negligible CTs indicate that these 32CA reactions have a non-polar character.

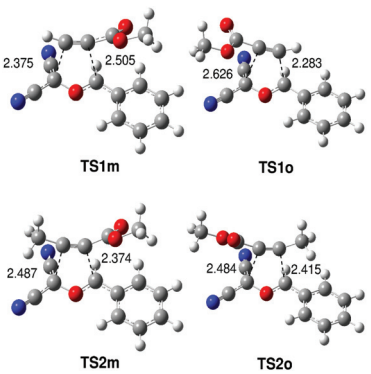

Fig. 1 Transition structures involved in the reactions between CY **1′a** and methyl propiolate (**4**) and methyl but-2-ynoate (**6**) (distances are given in Å).

Analysis based on the global reactivity indices at the ground state of the reagents

Studies devoted to Diels–Alder and 32CA reactions have shown that the analysis of the global indices defined within the context of conceptual DFT[15] is a powerful tool to understand the behavior of polar cycloadditions.[16] In Table 5, we report the static global properties, namely, electronic chemical potential μ, chemical hardness η, global electrophilicity ω and nucleophilicity N of the CY **1′a** and methyl propiolate (**4**) and methyl but-2-ynoate (**6**).

The electronic chemical potential μ of methyl propiolate (**4**), μ = −4.42 eV, and methyl but-2-ynoate (**6**), μ = −4.04 eV, is slightly higher than that for the CY **1′a**, −4.61 eV. The gaps of electronic chemical potentials between reagents, $\Delta\mu$, are below 0.6 eV. These low values do not permit to establish a tendency for the flux of the CT along the cycloaddition, in clear agreement with the NBO analysis at the corresponding TSs.

The CY **1′a** has a high electrophilicity value, ω = 4.29 eV, being classified as a strong electrophile in the electrophilicity scale. On the other hand, the CY **1′a** also has a very high nucleophilicity value, N = 3.28 eV, also being classified as a strong nucleophile in the nucleophilicity scale. Consequently, the CY **1′a** can act as a strong electrophile towards nucleophilic species and as a strong nucleophile towards electrophilic species.

Methyl propiolate (**4**) and methyl but-2-ynoate (**6**) present low electrophilicity values, ω = 1.52 and 1.29 eV, respectively, being classified as moderate electrophiles. On the other hand, they have somewhat low nucleophilicity values, N = 1.48 and 1.92 eV, respectively, being also classified as poor nucleophiles. As expected, the methyl substitution in methyl but-2-ynoate (**6**) decreases the electrophilicity and increases the nucleophilicity of methyl propiolate (**4**).

Analysis of the reactivity indices indicates that although the CY **1′a** can participate in polar 32CA reactions as a consequence of its high electrophilic and nucleophilic character, the low electrophilic and nucleophilic power of methyl propiolate (**4**) and methyl but-2-ynoate (**6**) prevent their participation in polar

Table 5 Electronic chemical potential (μ, in au), chemical hardness (η, in au), global electrophilicity (ω, in eV) and global nucleophilicity (N, in eV) values of CY **1′a** and methyl propiolate (**4**) and methyl but-2-ynoate (**6**)

	μ	η	ω	N
1′a	−4.61	2.47	4.29	3.28
4	−4.42	6.43	1.52	1.48
6	−4.04	6.32	1.29	1.92

cycloadditions. The behavior of the alkynes **4** and **6** could be responsible for the low CT observed at the corresponding TSs.

ELF topological analysis of the 32CA reaction between the CY 1′a and methyl propiolate (4)

Recent theoretical studies have shown that the topological analysis of the ELF along the reaction path associated with a cycloaddition is a valuable tool for understanding the bonding changes along the reaction path.[17] Consequently, a topology analysis of the ELF of some selected points along the most favorable reaction path associated with the 32CA reaction between the CY **1′a** and methyl propiolate (**4**) was performed in order to understand the bond-formation in these 32CA reactions. The *N* populations of the most relevant ELF valence basins are listed in Table 6. A schematic picture of the attractor positions and atom numbering is shown in Fig. 2.

ELF analysis of the CY **1′a** shows two disynaptic basins V(C1,O2) and V(O2,C3), whose electronic populations integrate 1.69e and 2.14e, respectively, one monosynaptic basin V(O2) integrating 3.57e, and two monosynaptic basins V(C1) and V′(C1), integrating 1.17e. Recently, we studied the non-polar 32CA reaction between the CY **13** and tetramethylethylene (**14**) (see Scheme 3).[17d] ELF analysis of the CY **13** showed two pairs of monosynaptic basins V(Cx) and V′(Cx) at each C2 and C2′ carbon, integrating *ca*. 1.0e each pair, and one monosynaptic basin V(O1) integrating 3.58e. The high reactivity of the CY **13** towards unactivated tetramethylethylene (**14**) was attributed to its *pseudodiradical* electronic structure, which allows for the C–C bond formation. Note that the activation enthalpy associated with this non-polar 32CA reaction was only 4.7 kcal mol^{-1}.[17d] The absence of the two monosynaptic basins at the C3 carbon of the CY **1′a** can be explained by a delocalization of the electron density of this *pseudodiradical* center at the adjacent phenyl group. This delocalization is supported by the changes of electron density of the disynaptic basin V(C3,C6) along the IRC, which decreases from 2.79e in CY **1′a** to 2.05e in **CA1m**.

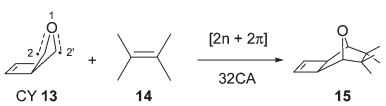

Scheme 3

On the other hand, methyl propiolate (**4**) has two disynaptic basins V(C4,C5) and V′(C4,C5), integrating 5.40e. These disynaptic basins account for the C4–C5 triple bond drawn in the Lewis structure of methyl propiolate (**4**).

Along the 32CA pathway, the ELF analysis of **TS1m**, d_1 = 2.375 Å and d_2 = 2.505 Å, shows that while the two monosynaptic basins V(C1) and V′(C1) have merged into one monosynaptic basin V(C1), integrating 0.90e, a new monosynaptic basin V(C4), integrating 0.35e, has been created at the C4 carbon of methyl propiolate (**4**). Simultaneously, the two disynaptic basins V(C4,C5) and V′(C4,C5) belonging to the C4–C5 triple bond region of **4** have been depopulated by *ca.* 0.40e. At this point of the IRC, the CT is very low, 0.05e. This low value indicates that this cycloaddition has no polar character. Unlike polar cycloadditions in which monosynaptic basins appear at the most electrophilic center of the electrophile as a consequence of the CT which takes place along the nucleophilic attack, in the present non-polar cycloaddition, the monosynaptic basin V(C4) appears as a consequence of the internal electron reorganization that takes place at the C4–C5 triple bond region along the reaction path.

At **P1**, d_1 = 2.075 Å and d_2 = 2.255 Å, while the monosynaptic basin V(C1) has slightly increased its population, the monosynaptic basin V(C4) has reached 0.71e. Additionally, at this point of the IRC two monosynaptic basins V(C3) and V(C5),

Table 6 Valence basin populations *N* calculated from the ELF of some selected points of the IRC associated with the most favorable regioisomeric channel of the 32CA reaction between CY **1′a** and methyl propiolate (**4**). The CT is also included

	1′a + 4	TS1m	P1	P2	CA1m
d1(C1–C5)		2.375	2.075	1.767	1.523
d2(C3–C4)		2.505	2.255	1.922	1.515
CT(NBO)		0.05	0.07	0.07	
CT(ELF)		0.06	0.07	0.08	
V(C1,O2)	1.69	1.54	1.44	1.34	1.24
V(O2)	3.57	3.95	4.38	2.49	2.59
V′(O2)				2.26	2.45
V(O2,C3)	2.14	1.91	1.62	1.41	1.22
V(C3,C6)	2.79	2.69	2.35	2.17	2.05
V(C4,C5)	2.70	2.51	2.17	1.94	1.84
V′(C4,C5)	2.70	2.47	2.17	1.96	1.74
V(C1)	0.59	0.90	1.05		
V′(C1)	0.58				
V(C3)			0.46		
V(C4)		0.35	0.71		
V(C5)			0.42		
V(C1,C5)				1.79	1.97
V(C3,C4)				1.69	2.04

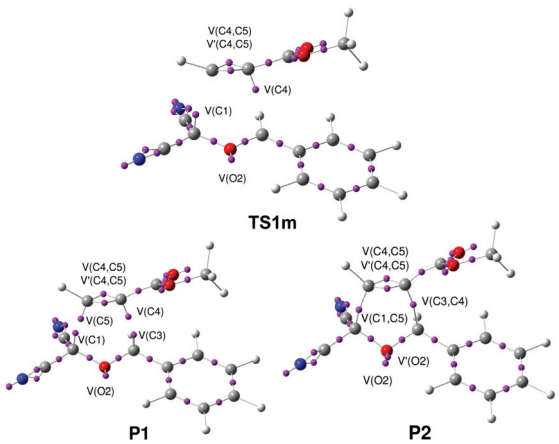

Fig. 2 ELF attractors at selected points of the IRC associated with the 32CA reaction between CY **1′a** and methyl propiolate (**4**).

integrating 0.46e and 0.42e respectively, have been created at the C3 carbon of the CY **1′a** and at C5 carbon of **4**. Simultaneously, the C4–C5 triple bond region has been depopulated by 0.64e. At **P2**, d_1 = 1.767 Å and d_2 = 1.922 Å, the four monosynaptic basins V(C1) and V(C5), and V(C3) and V(C4), have merged into two new disynaptic basins, V(C1,C5) and V(C3, C4), which integrate 1.79e and 1.69e, respectively. Consequently, at this point of the IRC, the two new C1–C5 and C3–C4 σ bonds have already been formed. At **P2**, while the populations of the two disynaptic basins V(C4,C5) and V′(C4,C5) have decreased to 1.94e and 1.96e, the monosynaptic basin V(O2) present in the CY **1′a** has split into two monosynaptic basins V(O2) and V′(O2), integrating 2.49e and 2.26e. Finally, **CA1m**, d_1 = 1.523 Å and d_2 = 1.515 Å, presents a similar bonding pattern to that at **P2**. As shown in Table 6, only slight changes in the basin populations take place at the end of the reaction.

The ELF bonding analysis at **TS1m** indicates that the main change in the electronic structure of methyl propiolate (**4**) is associated with the formation of a C4 *pseudoradical* center. Note that at the CY **1′a**, only the fusion of the two monosynaptic basins V(C1) and V′(C1) into the monosynaptic basin V(C1) takes place. This change is associated with the depopulation in electron density at the C4–C5 triple bond region. This behavior together with the very low CT at **TS1m**, 0.06e (ELF) and 0.05 (NBO), suggests a non-polar 32CA reaction with a *pseudodiradical* character. Recently, we established that the high reactivity of CYs in non-polar processes can be associated with their *pseudodiradical* character, which enables the reaction to take place through an unappreciable barrier.[17d]

Finally, ELF bonding analysis at the C1–O2–C3 framework of the CY **1′a** along the 32CA reaction shows that while the electron density of the monosynaptic basins V(O2) and V′(O2) increases from 3.57e in the CY **1′a** to 5.04 e in **CA1m**, the electron density of the disynaptic basins V(C1,O2) and V(O2,C3) decreases from 3.83e in the CY **1′a** to 2.46e in **CA1m**. This behavior, which is similar to that found in the non-polar 32CA reaction between the CY **13** and tetramethylethylene (**14**) in Scheme 3,[17d] indicates that the O2 lone pairs of the CY **1′a** do not participate in the C–C bond formation in the 32CA reaction; while in the CY **1′a** these O2 lone pairs are partially delocated in the *pseudoradical* C1 and C3 centers, in **CA1m** they are mainly located at the O2 oxygen as a consequence of the saturation of the C1 and C3 carbons after the C–C bond formations. This behavior allows for the establishment that these 32CA reactions may be electronically classified as [$2n + 2\pi$] processes,[17c,d] in which only the two electrons of the HOMO of the CY **1′a** and the two electrons of the HOMO − 1 of methyl propiolate (**4**) participate in the 32CA reaction (see Fig. 3).

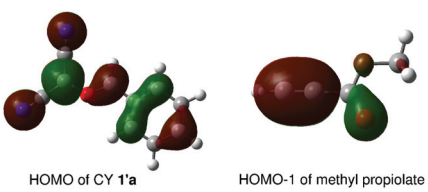

Fig. 3 HOMO of CY **1′a** and the two electrons of HOMO − 1 of methyl propiolate (**4**).

What is the origin of the regioselectivity in these non-polar 32CA reactions?

While Diels–Alder reactions present a high regioselectivity, which increases with the polar character of the reaction,[18] 32CA reactions present a low regioselectivity, which also depends on polarity. Thus, it is expected that these non-polar 32CA reactions will have a poor regioselectivity. However, both experimental and theoretical calculations show that both reactions are regioselective. Analyses of the local reactivity indices indicate that the C1 carbon of the CY **1′a** is the most nucleophilic center,[7] and that the β conjugated C5 position of methyl propiolate (**4**) and methyl but-2-ynoate (**6**) is the most electrophilic center of these molecules. Therefore, although the polar analysis explains the observed regioselectivity, the bonding pattern involved in polar cycloadditions cannot rule in these non-polar 32CA reactions.[19]

ELF analysis of the electronic structures of the four TSs involved in these non-polar 32CA reactions allows us to obtain some interesting information. For simplicity, only the ELF attractors of the four TSs are given in Fig. 4. The four TSs show two monosynaptic basins, the V(C1) and the V(C4) at the regioisomeric **TS1m** and **TS2m**, and the V(C1) and the V(C5) at the regioisomeric **TS1o** and **TS2o**. Therefore, the four TSs share the presence of the monosynaptic basin V(C1), which is already present in the CY **1′a** with similar population, and the monosynaptic basins V(C4) in channels **m** and the V(C5) in channels **o**, which are created along the reaction. Interestingly, in the four TSs, the first monosynaptic basin at the acetylenic system appears at the opposite carbon of the CY, regardless of the carbonyl group position. Note that in a polar cycloaddition, these basins appear always at the β conjugated position, which correspond with the most electrophilic center of these acetylene derivatives.[19] Consequently, we can associate the relative stability of the two pairs of regioisomeric TSs with the relative stability of the corresponding *pseudodiradical* species formed on going to the corresponding TS. Unlike the polar cycloadditions in which the formation of the monosynaptic basins takes place firstly at the β conjugated position, in these non-polar 32CA

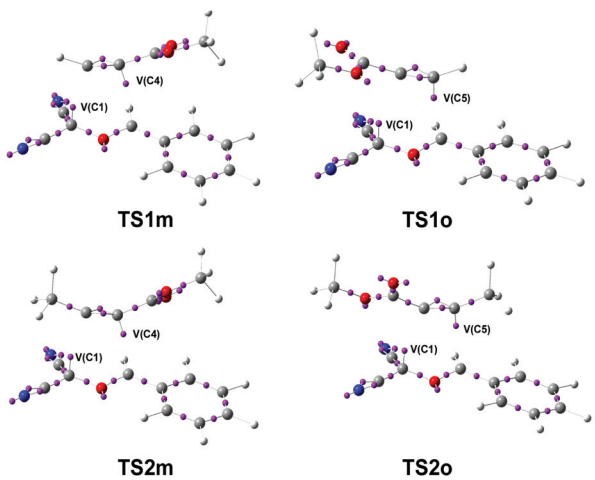

Fig. 4 ELF attractors at the TSs involved in the non-polar 32CA reactions between CY **1′a** and methyl propiolate (**4**) and methyl but-2-ynoate (**6**).

reactions the formation of the monosynaptic basin at the α position appears to be favored over the β one. This finding could explain the larger regioselectivity found in the 32CA reaction using methyl but-2-ynoate (**6**) than that with methyl propiolate (**4**). The presence of the electron-releasing methyl group on C5 carbon of but-2-ynoate (**6**) favors the formation of monosynaptic basin V(C4) in **TS2m** with respect to **TS1m**. This behavior is supported by the larger population of the monosynaptic basin V(C4) in **TS2m**, 0.58e, than that in **TS1m**, 0.35e. Note that in both TSs, the monosynaptic basin V(C1) presents the same population, 0.90e.

Pharmacology

Applying the agar plate diffusion technique,[20] the newly synthesized compounds **3a**, **5′c** and **9c** were screened *in vitro* for their bactericidal activity against Gram positive bacteria (*Staphylococcus aureus*) and Gram negative bacteria (*Escherichia coli* and *Pseudomonas aeroginosa*), and for their fungicidal activity towards *Fusarium oxysporium*, *Aspergillus niger* and *Candida albicans* (Table 7). All the compounds tested showed moderate bactericidal activities against *Staphylococcus aureus*, *Escherichia coli* and *Pseudomonas aeroginosa* compared to that of ciprofloxacin as a reference drug. The compounds tested showed moderate fungicidal activities towards *Fusarium oxysporium* and *Aspergillus niger* compared to that of nystin as a reference, except the compound **5′c** that showed significant activities, in particular against *Fusarium oxysporium*. Only the compound **5′c** showed a moderate activity against *Candida albicans*.

The compounds **3a,b**, **5′c** and **9c** were also tested against a human liver carcinoma cell line (HEPG2), and **3b** against human breast (MCF7) and cervix (HELA) carcinoma cell lines (Table 8). Moderate cytotoxic activities were observed for all the compounds tested, compared to a reference drug (doxorubicin), except in the case of **3b**, for which activities close to those of doxorubicin were observed. The difference in the value of IC_{50} between the two compounds **3a** and **3b** may be due to the presence of the chloro group in **3b**, a substituent that can affect the biological activity of the compounds.[21]

Conclusions

Thus, substituted 2,5-dihydrofurans were synthesized by the 32CA reaction between carbonyl ylides generated from epoxides and alkynes. While 3-phenyl-5-(4-substituted phenyl)-(2*H*,5*H*)-dihydrofuran-2,2-dicarbonitrile **3** and methyl 2,2-dicyano-5-(4-substituted phenyl)-(2*H*,5*H*)-dihydrofuran-4-carboxylate **5′** only dominate using phenylacetylene (**2**) and methyl propiolate (**4**), respectively, the use of methyl but-2-ynoate (**6**) and methyl 3-phenylpropiolate (**7**) led to only one regioisomer, the methyl 5-(4-substituted phenyl)-2,2-dicyano-(2*H*,5*H*)-dihydrofuran-4-carboxylates **8** and **9**, respectively methylated or phenylated at C3. The different observed regioisomeric ratios using methyl propiolate (**4**) and methyl but-2-ynoate (**6**) in the reactions with the CY **1′a** were explained by theoretical calculations.

Despite the high electrophilic and nucleophilic character of the CY **1′a**, the low electrophilic and nucleophilic character of the alkynes **4** and **6** causes these 32CA reactions to take place through a non-polar mechanism *via* TSs with a *pseudodiradical* character. In spite of the low activation energy associated with these non-polar 32CA reactions, the endothermic character associated with the formation of the CY **1′a** was found to be responsible for the high temperature required to carry out these thermal reactions. Finally, analysis of the bonding changes along these 32CA reactions allows for the classification of these non-polar cycloadditions as [2*n* + 2π] processes.

Experimental

Syntheses: general methods

Liquid chromatography separations were achieved on silica gel Merck–Geduran Si 60 (40–63 μm). Petrol refers to petroleum ether (bp 40–60 °C). Melting points were measured on a Kofler apparatus. Nuclear magnetic resonance spectra were acquired using a Bruker AC-300 spectrometer (300 MHz and 75 MHz for ^{1}H and ^{13}C respectively). ^{1}H chemical shifts (δ) are given in

Table 8 *In vitro* cytotoxic activity (IC_{50})[a] of the compounds **3a,b**, **5′c**, **9c**, and doxorubicin against carcinoma cell lines

Entry	Compound	HEPG2 (μg mL^{-1})	MCF7 (μg mL^{-1})	HELA (μg mL^{-1})
1	**3a**	2.88	—	—
2	**3b**	0.67	0.74	0.89
3	**5′c**	2.98	—	—
4	**9c**	3.34	—	—
5	Doxorubicin	0.60	0.70	0.85

[a] IC_{50} is defined as the concentration which results in a 50% decrease in the cell number as compared with that of the control structures in the absence of an inhibitor.

Table 7 Bactericidal and fungicidal activity[a] of the compounds **3a**, **5′c**, **9c**, and ciprofloxacin and nystin

Entry	Compound	*Staphylococcus aureus*	*Escherichia coli*	*Pseudomonas aeroginosa*	*Fusarium oxysporium*	*Aspergillus niger*	*Candida albicans*
1	**3a**	19 (++)	17 (++)	17 (++)	19 (++)	20 (++)	—
2	**5′c**	27 (+++)	15 (++)	22 (++)	43 (++++)	27 (+++)	18 (++)
3	**9c**	18 (++)	17 (++)	16 (++)	16 (++)	18 (++)	—
4	Ciprofloxacin	++++	++++	++++	—	—	—
5	Nystin	—	—	—	++++	++++	++++

[a] The diameters of zones of inhibition are given in mm. Stock solution: 5 μg in 1 mL of DMF. 0.1 mL of stock solution in each hole of each paper disk. +: <15 mm; ++: 15–24 mm; +++: 25–34 mm; ++++: 35–44 mm, *etc.*

ppm relative to the solvent residual peak, and ^{13}C chemical shifts relative to the central peak of the solvent signal. NOESY, HMBC and HMQC experiments were performed on an Avance 500 spectrometer (500 MHz and 125 MHz for ^{1}H and ^{13}C, respectively). High resolution mass spectra measurements were recorded at the Centre Régional de Mesures Physiques de l'Ouest (CRMPO) in Rennes. Oxiranes were prepared according to the described procedures.[9] Toluene was dried before use. Reactions were performed under dry argon.

General procedure 1. A mixture of epoxide (2 mmol) and phenylacetylene (1.0 g, 10 mmol) in anhydrous toluene (30 mL) was heated at reflux under Ar for 40 h. The mixture was then evaporated to dryness and the product isolated by column chromatography over silica gel (eluent: 25 : 75 CH_2Cl_2–petrol).

General procedure 2. A mixture of epoxide (2 mmol), phenylacetylene (0.80 g, 8 mmol) and $InCl_3$ (40 mg, 0.2 mmol) in anhydrous toluene (30 mL) was heated at reflux under Ar for 29 h (**1a**), 27 h (**1b**) and 20 h (**1c**). The mixture was then evaporated to dryness and the product isolated by column chromatography over silica gel (eluent: 25 : 75 CH_2Cl_2–petrol).

*3,5-Diphenyl-(2*H*,5*H*)-dihydrofuran-2,2-dicarbonitrile (**3a**).* Yield: 40% (general procedure 1), 60% (general procedure 2). White powder, mp 133 °C. ^{1}H NMR (300 MHz, $CDCl_3$): 6.25 (d, 1H, J = 1.8 Hz), 6.65 (d, 1H, J = 1.8 Hz), 7.36–7.39 (m, 2H), 7.43–7.48 (m, 3H), 7.48–7.50 (m, 3H), 7.65–7.68 (m, 2H). ^{13}C NMR (75 MHz, $CDCl_3$): 73.8, 91.6, 113.1, 113.2, 126.8 (2C), 127.0 (2C), 127.5, 129.3 (2C), 129.5 (2C), 129.8, 130.5, 131.0, 134.6, 136.5. HRMS (ESI): calcd for $C_{18}H_{12}N_2O$ ($M^{+\cdot}$) 272.0842, found 272.0842.

*5-(4-Chlorophenyl)-3-phenyl-(2*H*,5*H*)-dihydrofuran-2,2-dicarbonitrile (**3b**).* Yield: 52% (general procedure 1), 64% (general procedure 2). Yellow powder, mp 85 °C. ^{1}H NMR (300 MHz, $CDCl_3$): 6.22 (d, 1H, J = 1.8 Hz), 6.62 (d, 1H, J = 1.8 Hz), 7.30 (d, 2H, J = 8.4 Hz), 7.42 (d, 2H, J = 8.4 Hz), 7.46–7.50 (m, 3H), 7.63–7.67 (m, 2H). ^{13}C NMR (75 MHz, $CDCl_3$): 73.7, 90.7, 112.8, 113.1, 126.8 (2C), 127.2, 128.4 (2C), 129.5 (2C), 129.6 (2C), 130.5, 130.7, 134.9, 135.0, 135.7. HRMS (ESI): calcd for $C_{18}H_{11}{}^{35}ClN_2O$ ($M^{+\cdot}$) 306.0576, found 306.0455.

*5-(4-Chlorophenyl)-4-phenyl-(2*H*,5*H*)-dihydrofuran-2,2-dicarbonitrile (**3'b**).* Yield: 12% (general procedure 1). Pale yellow oil. ^{1}H NMR (300 MHz, $CDCl_3$): 6.33 (d, 1H, J = 2.1 Hz), 6.41 (d, 1H, J = 2.1 Hz), 7.26–7.29 (m, 2H), 7.29–7.32 (m, 3H), 7.34–7.37 (m, 4H). ^{13}C NMR (75 MHz, $CDCl_3$): 72.6, 91.1, 112.7, 113.0, 127.3, 127.5 (2C), 129.1, 129.2 (2C), 129.6 (2C), 129.6, 129.7 (2C), 130.9, 134.6, 136.1. HRMS (ESI): calcd for $C_{18}H_{11}{}^{35}ClN_2O$ ($M^{+\cdot}$) 306.0576, found 306.0459.

*5-(4-Methoxyphenyl)-3-phenyl-(2*H*,5*H*)-dihydrofuran-2,2-dicarbonitrile (**3c**).* Yield: 50% (general procedure 1), 60% (general procedure 2). Yellow powder, mp 118 °C. ^{1}H NMR (300 MHz, $CDCl_3$): 3.83 (s, 3H), 6.20 (d, 1H, J = 1.8 Hz), 6.62 (d, 1H, J = 1.8 Hz), 6.94–6.97 (m, 2H), 7.27–7.31 (m, 2H), 7.47–7.50 (m, 3H), 7.64–7.67 (m, 2H). ^{13}C NMR (75 MHz, $CDCl_3$): 55.5, 73.5, 91.4, 113.1, 113.3, 114.6 (2C), 126.8 (2C), 127.6, 128.5, 128.8 (2C), 129.5 (2C), 130.5, 131.0, 134.6, 160.8. HRMS (ESI): calcd for $C_{19}H_{14}N_2O_2$ [$(M + Na)^{+\cdot}$] 302.0953, found 302.0953.

General procedure 3. A mixture of epoxide (2 mmol) and methyl propiolate (0.67 g, 8 mmol in the case of **1a,b**; 0.16 g, 2 mmol in the case of **1c**) in anhydrous toluene (30 mL) was heated at reflux under Ar for 48 h (**1a,b**) or 24 h (**1c**). The mixture was then evaporated to dryness and the product isolated by column chromatography over silica gel (eluent: 10 : 90 AcOEt–petrol in the case of **1a,b**; 20 : 80 with **1c**).

General procedure 4. A mixture of epoxide (2 mmol), methyl propiolate (0.67 g, 8 mmol in the case of **1a,b**; 0.16 g, 2 mmol in the case of **1c**) and $InCl_3$ (40 mg, 0.2 mmol) in anhydrous toluene (30 mL) was heated at reflux under Ar for 36 h (**1a,b**) or 20 h (**1c**). The mixture was then evaporated to dryness and the product isolated by column chromatography over silica gel (eluent: 10 : 90 AcOEt–petrol in the case of **1a,b**; 20 : 80 with **1c**).

*Methyl 2,2-dicyano-5-phenyl-(2*H*,5*H*)-dihydrofuran-3-carboxylate (**5a**).* Yield: 12% (general procedure 3). Yellow oil. ^{1}H NMR (300 MHz, $CDCl_3$): 3.95 (s, 3H), 6.27 (d, 1H, J = 1.8 Hz), 7.26 (d, 1H, J = 1.8 Hz), 7.29–7.32 (m, 3H), 7.42–7.45 (m, 2H). ^{13}C NMR (75 MHz, $CDCl_3$): 53.4, 72.4, 91.7, 112.0, 112.3, 126.9 (2C), 128.1, 130.2 (2C), 130.2, 134.6, 146.7, 159.1. HRMS (ESI): calcd for $C_{14}H_{10}N_2O_3$ ($M^{+\cdot}$) 254.0589, found 254.0592.

*Methyl 2,2-dicyano-5-phenyl-(2*H*,5*H*)-dihydrofuran-4-carboxylate (**5'a**).* Yield: 40% (general procedure 3), 58% (general procedure 4). White powder, mp 102 °C. ^{1}H NMR (300 MHz, $CDCl_3$): 3.73 (s, 3H), 6.24 (d, 1H, J = 2.1 Hz), 6.78 (d, 1H, J = 2.1 Hz), 7.32–7.35 (m, 2H), 7.41–7.43 (m, 3H). ^{13}C NMR (75 MHz, $CDCl_3$): 53.0, 72.3, 91.1, 111.6, 111.8, 127.6 (2C), 128.7, 129.1 (2C), 130.1, 135.1, 142.9, 160.2. HRMS (ESI): calcd for $C_{14}H_{10}N_2O_3$ ($M^{+\cdot}$) 254.0589, found 254.0593.

*Methyl 5-(4-chlorophenyl)-2,2-dicyano-(2*H*,5*H*)-dihydrofuran-3-carboxylate (**5b**).* Yield: 10% (general procedure 3). Yellow oil. ^{1}H NMR (300 MHz, $CDCl_3$): 3.96 (s, 3H), 6.24 (d, 1H, J = 1.8 Hz), 7.23 (d, 1H, J = 1.8 Hz), 7.24–7.27 (m, 2H), 7.40–7.43 (m, 2H). ^{13}C NMR (75 MHz, $CDCl_3$): 54.5, 72.4, 90.8, 111.9, 112.2, 128.3 (2C), 128.6, 129.8 (2C), 133.1, 136.3, 146.0, 159.0. HRMS (APCI/ASAP): calcd for $C_{14}H_8{}^{35}ClN_2O_3$ [$(M - H)^{+\cdot}$] 287.0218, found 287.0222.

*Methyl 5-(4-chlorophenyl)-2,2-dicyano-(2*H*,5*H*)-dihydrofuran-4-carboxylate (**5'b**).* Yield: 54% (general procedure 3), 57% (general procedure 4). White powder, mp 105 °C. ^{1}H NMR (300 MHz, $CDCl_3$): 3.75 (s, 3H), 6.21 (d, 1H, J = 2.1 Hz), 6.78 (d, 1H, J = 2.1 Hz), 7.26–7.29 (m, 2H), 7.39–7.41 (m, 2H). ^{13}C NMR (75 MHz, $CDCl_3$): 53.1, 72.3, 90.3, 111.4, 111.7, 128.9, 129.0 (2C), 129.5 (2C), 133.7, 136.2, 142.6, 160.0. HRMS (APCI/ASAP): calcd for $C_{14}H_8{}^{35}ClN_2O_3$ [$(M - H)^{+\cdot}$] 287.0218, found 287.0219.

*Methyl 2,2-dicyano-5-(4-methoxyphenyl)-(2*H*,5*H*)-dihydrofuran-3-carboxylate (**5c**).* Yield: 11% (general procedure 3), 8% (general procedure 4). Yellow oil. ^{1}H NMR (300 MHz, $CDCl_3$): 3.82 (s, 3H), 3.96 (s, 3H), 6.22 (d, 1H, J = 1.5 Hz), 6.93–6.96 (m, 2H), 7.20–7.23 (m, 2H), 7.24 (d, 1H, J = 1.5 Hz). ^{13}C NMR (75 MHz, $CDCl_3$): 53.4, 55.5, 72.0, 91.5, 112.1, 112.4, 114.8 (2C), 126.4, 128.2, 128.8 (2C), 146.7, 159.2, 161.1. NMR HMQC sequences performed on **5c** showed relationship between H4 and C5 (see Table 2). HRMS (ESI): calcd for $C_{15}H_{12}N_2O_4$ ($M^{+\cdot}$) 284.0689, found 284.0683.

*Methyl 2,2-dicyano-5-(4-methoxyphenyl)-(2H,5H)-dihydrofuran-4-carboxylate (**5′c**).* Yield: 65% (general procedure 3), 67% (general procedure 4). Yellow oil. ^{1}H NMR (300 MHz, $CDCl_3$): 3.71 (s, 3H), 3.79 (s, 3H), 6.19 (d, 1H, J = 2.1 Hz), 6.77 (d, 1H, J = 2.1 Hz), 6.91–6.94 (m, 2H), 7.23–7.26 (m, 2H). ^{13}C NMR (75 MHz, $CDCl_3$): 52.9, 55.4, 71.9, 90.8, 111.6, 111.9, 114.5 (2C), 127.1, 128.5, 129.1 (2C), 142.7, 160.2, 160.8. NMR HMQC sequences performed on **5′c** showed relationship between the phenyl protons and the carbonyl group. HRMS (ESI): calcd for $C_{15}H_{12}N_2O_4$ ($M^{+\cdot}$) 284.0689, found 284.0689.

General procedure 5. A mixture of epoxide (2 mmol) and methyl but-2-ynoate (2.1 g, 22 mmol in the case of **1a,b**; 1.6 g, 16 mmol in the case of **1c**) in anhydrous toluene (30 mL) was heated at reflux under Ar for 48 h (**1a,b**) or 24 h (**1c**). The mixture was then evaporated to dryness and the product isolated by column chromatography over silica gel (eluent: 5 : 95 AcOEt–petrol in the case of **1a,b**; 10 : 90 with **1c**) followed by recrystallization in CH_2Cl_2.

*Methyl 2,2-dicyano-3-methyl-5-phenyl-(2H,5H)-dihydrofuran-4-carboxylate (**8a**).* Yield: 66% (general procedure 5). Yellow powder, mp 83 °C. ^{1}H NMR (300 MHz, $CDCl_3$): 2.44 (d, 3H, J = 2.10 Hz), 3.68 (s, 3H), 6.20 (q, 1H, J = 2.10 Hz), 7.28–7.31 (m, 2H), 7.39–7.41 (m, 3H). ^{13}C NMR (75 MHz, $CDCl_3$): 11.2, 52.5, 77.2, 92.2, 111.9, 112.0, 127.7 (2C), 129.0 (2C), 129.9, 134.1, 136.1, 140.4, 161.4. HRMS (APCI/ASAP): calcd for $C_{15}H_{11}N_2O_3$ [$(M - H)^{+\cdot}$] 267.0764, found 267.0765.

*Methyl 5-(4-chlorophenyl)-2,2-dicyano-3-methyl-(2H,5H)-dihydrofuran-4-carboxylate (**8b**).* Yield: 62% (general procedure 5). White powder, mp 105 °C. ^{1}H NMR (300 MHz, $CDCl_3$): 2.45 (d, 3H, J = 2.10 Hz), 3.70 (s, 3H), 6.18 (q, 1H, J = 2.10 Hz), 7.23–7.26 (m, 2H), 7.37–7.40 (m, 2H). ^{13}C NMR (75 MHz, $CDCl_3$): 11.2, 52.6, 77.1, 91.3, 111.7, 111.9, 129.0 (2C), 129.3 (2C), 133.7, 134.6, 135.9, 140.8, 161.2. HRMS (APCI/ASAP): calcd for $C_{15}H_{10}{}^{35}ClN_2O_3$ [$(M - H)^{+\cdot}$] 301.0374, found 301.0375.

*Methyl 2,2-dicyano-5-(4-methoxyphenyl)-3-methyl-(2H,5H)-dihydrofuran-4-carboxylate (**8c**).* Yield: 44% (general procedure 5). Yellow oil. ^{1}H NMR (300 MHz, $CDCl_3$): 2.43 (d, 3H, J = 2.10 Hz), 3.67 (s, 3H), 3.79 (s, 3H), 6.16 (q, 1H, J = 2.10 Hz), 6.89–6.92 (m, 2H), 7.21–7.24 (m, 2H). ^{13}C NMR (75 MHz, $CDCl_3$): 11.1, 52.4, 55.3, 76.8, 91.8, 111.9, 112.1, 114.3 (2C), 128.1, 129.0 (2C), 134.0, 140.0, 160.7, 161.4. An NMR HMQC sequence performed on **8c** showed a relationship between the methyl group protons connected to the dihydrofuran ring and the nitrile functions, in accordance with a methyl at C3 (see Table 3). HRMS (ESI): calcd for $C_{16}H_{14}N_2O_4$ ($M^{+\cdot}$) 298.0846, found 298.0848.

General procedure 6. A mixture of epoxide (2 mmol) and methyl 3-phenylpropiolate (0.32 g, 2 mmol) in anhydrous toluene (30 mL) was heated at reflux under Ar for 96 h (**1a,b**) or 55 h (**1c**). The mixture was then evaporated to dryness and the product isolated by column chromatography over silica gel (eluent: 5 : 95 AcOEt–petrol in the case of **1a,b**; 10 : 90 with **1c**) followed by recrystallization in CH_2Cl_2.

*Methyl 2,2-dicyano-3,5-diphenyl-(2H,5H)-dihydrofuran-4-carboxylate (**9a**).* Yield: 60% (general procedure 6). Yellow powder, mp 85 °C. ^{1}H NMR (300 MHz, $CDCl_3$): 3.53 (s, 3H), 6.40 (s, 1H), 7.44–7.46 (m, 5H), 7.52–7.56 (m, 3H), 7.60–7.63 (m, 2H). ^{13}C NMR (75 MHz, $CDCl_3$): 52.6, 76.9, 92.2, 112.0, 112.2, 127.0, 127.7 (2C), 128.8 (2C), 129.1 (2C), 129.2 (2C), 130.1, 131.1, 135.7, 136.0, 140.2, 161.1. HRMS (APCI/ASAP): calcd for $C_{20}H_{13}N_2O_3$ [$(M - H)^{+\cdot}$] 329.0920, found 329.0924.

*Methyl 5-(4-chlorophenyl)-2,2-dicyano-3-phenyl-(2H,5H)-dihydrofuran-4-carboxylate (**9b**).* Yield: 47% (general procedure 6). White powder, mp 142 °C. ^{1}H NMR (300 MHz, $CDCl_3$): 3.53 (s, 3H), 6.36 (s, 1H), 7.35–7.38 (m, 2H), 7.42–7.45 (m, 2H), 7.50–7.60 (m, 5H). ^{13}C NMR (75 MHz, $CDCl_3$): 52.7, 76.7, 91.4, 111.8, 112.1, 126.8, 128.8 (2C), 129.1 (2C), 129.2 (2C), 129.5 (2C), 131.2, 134.3, 135.5, 136.2, 140.7, 161.0. HRMS (APCI/ASAP): calcd for $C_{20}H_{12}{}^{35}ClN_2O_3$ [$(M - H)^{+\cdot}$] 363.0531, found 363.0526.

*Methyl 2,2-dicyano-5-(4-methoxyphenyl)-3-phenyl-(2H,5H)-dihydrofuran-4-carboxylate (**9c**).* Yield: 66% (general procedure 6). Yellow oil. ^{1}H NMR (300 MHz, $CDCl_3$): 3.53 (s, 3H), 3.83 (s, 3H), 6.35 (s, 1H), 6.95–6.98 (m, 2H), 7.34–7.37 (m, 2H), 7.51–7.55 (m, 3H), 7.60–7.63 (m, 2H). ^{13}C NMR (75 MHz, $CDCl_3$): 52.6, 55.4, 76.5, 91.9, 112.1, 112.2, 114.5 (2C), 127.0, 127.6, 128.7 (2C), 129.0 (2C), 129.2 (2C), 131.0, 135.9, 139.9, 160.9, 161.2. HRMS (ESI): calcd for $C_{12}H_{16}N_2O_4$ ($M^{+\cdot}$) 360.1002, found 360.1002.

Crystallography

Single crystals suitable for X-ray diffraction were grown after slow evaporation (several days at room temperature) of solutions of **3a**, **3b** and **3c** in CH_2Cl_2. The samples were studied with graphite monochromatized $Mo_{K\alpha}$ radiation (λ = 0.71073 Å). X-ray diffraction data were collected at T = 100(2) K for **3a,b**, at T = 150(2) K for **3c**, and at T = 200(2) K for **5′a**, **5b**, **8a,b**, using an APEXII Bruker-AXS diffractometer (**3a–c**, **5′a**, **5b**, **8b**) or a KappaCCD diffractometer (**8a**). The structure was solved by direct methods using the SIR97 program,[22] and then refined with full-matrix least-squares methods based on F^2 (SHELX-97)[23] with the aid of the WINGX program.[24] All non-hydrogen atoms were refined with anisotropic atomic displacement parameters. H atoms were finally included in their calculated positions. Molecular diagrams were generated by ORTEP-3 (version 1.08)[25] and furnished as ESI.†

Crystal data for 3a. $C_{18}H_{12}N_2O$, M = 272.30, monoclinic, $P2_1$, a = 7.7576(3), b = 6.0070(2), c = 14.7572(6) Å, β = 93.710(2)°, V = 686.24(4) Å^3, Z = 2, d = 1.32 g cm^{-3}, μ = 0.083 mm^{-1}. A final refinement on F^2 with 1721 unique intensities and 190 parameters converged at w$R(F^2)$ = 0.067 ($R(F)$ = 0.0275) for 1649 observed reflections with $I > 2\sigma(I)$.

Crystal data for 3b. $2(C_{18}H_{11}ClN_2O)$, M = 613.48, monoclinic, $P2_1/a$, a = 11.0917(5), b = 17.5158(6), c = 16.2080(6) Å, β = 109.615(2)°, V = 2966.2(2) Å^3, Z = 4, d = 1.37 g cm^{-3}, μ = 0.26 mm^{-1}. A final refinement on F^2 with 6660 unique intensities and 398 parameters converged at w$R(F^2)$ = 0.131 ($R(F)$ = 0.0449) for 6009 observed reflections with $I > 2\sigma(I)$.

Crystal data for 3c. $C_{19}H_{14}N_2O_2$, M = 302.32, triclinic, $P\bar{1}$, a = 7.446(4), b = 7.670(3), c = 15.675(11) Å, α = 97.60(4), β = 91.12(3), γ = 118.99(2)°, V = 772.5(7) Å^3, Z = 2, d =

1.30 g cm^{-3}, μ = 0.086 mm^{-1}. A final refinement on F^2 with 3395 unique intensities and 211 parameters converged at w$R(F^2)$ = 0.2758 ($R(F)$ = 0.0897) for 2690 observed reflections with $I > 2\sigma(I)$.

Crystal data for 5′a. $C_{14}H_{10}N_2O_3$, M = 254.24, orthorhombic, $P2_12_12_1$, a = 6.355(1), b = 8.010(1), c = 24.798(3) Å, V = 1262.4(3) Å^3, Z = 4, d = 1.34 g cm^{-3}, μ = 0.096 mm^{-1}. A final refinement on F^2 with 2876 unique intensities and 173 parameters converged at w$R(F^2)$ = 0.0921 ($R(F)$ = 0.0391) for 2380 observed reflections with $I > 2\sigma(I)$.

Crystal data for 5b. $C_{14}H_9ClN_2O_3$, M = 288.68, monoclinic, $P2_1/c$, a = 11.0681(3), b = 9.2126(3), c = 13.3847(3) Å, β = 90.0100(10)°, V = 1364.78(7) Å^3, Z = 4, d = 1.40 g cm^{-3}, μ = 0.288 mm^{-1}. A final refinement on F^2 with 3101 unique intensities and 182 parameters converged at $\omega R(F^2)$ = 0.0906 ($R(F)$ = 0.0372) for 2394 observed reflections with $I > 2\sigma(I)$.

Crystal data for 8a. $C_{15}H_{12}N_2O_3$, M = 268.27, monoclinic, $P2_1$, a = 8.5077(4), b = 9.6154(5), c = 9.3240(4) Å, β = 116.932(7)°, V = 680.02(6) Å^3, Z = 2, d = 1.31 g cm^{-3}, μ = 0.093 mm^{-1}. A final refinement on F^2 with 1659 unique intensities and 183 parameters converged at w$R(F^2)$ = 0.0784 ($R(F)$ = 0.0346) for 1509 observed reflections with $I > 2\sigma(I)$.

Crystal data for 8b. $C_{15}H_{11}ClN_2O_3$, M = 302.71, triclinic, $P\bar{1}$, a = 6.545(1), b = 10.072(2), c = 11.676(2) Å, α = 107.83(5), β = 101.23(4), γ = 92.80(3)°, V = 713.8(4) Å^3, Z = 2, d = 1.41 g cm^{-3}, μ = 0.279 mm^{-1}. A final refinement on F^2 with 3257 unique intensities and 192 parameters converged at w$R(F^2)$ = 0.0972 ($R(F)$ = 0.047) for 2050 observed reflections with $I > 2\sigma(I)$.

Computational methods

DFT calculations were carried out using the B3LYP[26] exchange–correlation functionals, together with the standard 6-31G* basis set.[27] All stationary points were further optimised using the 6-311G* and 6-311+G* basis sets. The corresponding results are given in the ESI† part. The optimisations were carried out using the Berny analytical gradient optimisation method.[28] The stationary points were characterized by frequency calculations in order to verify that TSs have one and only one imaginary frequency. The IRC[29] paths were traced in order to check the energy profiles connecting each TS to the two associated minima of the proposed mechanism using the second order González–Schlegel integration method.[30] Solvent effects were considered at the same level of theory by single-point energy calculations of the gas-phase structures using a self-consistent reaction field (SCRF)[31] based on the polarizable continuum model (PCM) of the Tomasi's group.[32] Since this cycloaddition was carried out in toluene, we selected its dielectric constant at 298.0 K, ε = 2.38. Values of enthalpies, entropies and free energies in toluene were calculated with standard statistical thermodynamics at 110 °C and 1 atm.[27] The electronic structures of stationary points were analyzed by the natural bond orbital (NBO) method[33] and by the topological analysis of the ELF, $\eta(r)$.[34] The ELF study was performed with the TopMod program[35] using the corresponding monodeterminantal wavefunctions of the selected structures of the IRC. All calculations were carried out with the Gaussian 09 suite of programs.[36]

The global electrophilicity index,[37] ω, is given by the following simple expression, $\omega = (\mu^2/2\eta)$, in terms of the electronic chemical potential μ and the chemical hardness η. Both quantities may be approached in terms of the one electron energies of the frontier molecular orbital HOMO and LUMO, ε_H and ε_L, as $\mu \approx (\varepsilon_H + \varepsilon_L)/2$ and $\eta \approx (\varepsilon_L - \varepsilon_H)$, respectively.[38] Recently, we have introduced an empirical (relative) nucleophilicity index,[39] N, based on the HOMO energies obtained within the Kohn–Sham scheme,[40] and defined as $N = E_{HOMO}(Nu) - E_{HOMO}(TCE)$. The nucleophilicity is referred to TCE, because it presents the lowest HOMO energy in a large series of molecules already investigated in the context of polar cycloadditions. This choice allows us conveniently to handle a nucleophilicity scale of positive values.[39]

Pharmacology

Applying the agar plate diffusion technique,[20] the compounds were screened *in vitro* for their bactericidal activity against Gram positive bacteria (*Staphylococcus aureus*) and Gram negative bacteria (*Escherichia coli* and *Pseudomonas aeroginosa*), and for their fungicidal activity against *Fusarium oxysporium*, *Aspergillus niger* and *Candida albicans*. In this method, a standard 5 mm diameter sterilized filter paper disc impregnated with the compound (0.3 mg per 0.1 ml of DMF) was placed on an agar plate seeded with the test organism. The plates were incubated for 24 h at 37 °C for bacteria and 28 °C for fungi. The zone of inhibition of bacterial and fungal growth around the disc was observed.

Compounds were tested against human liver (HEPG2), human breast (MCF7), and cervix (HELA) carcinoma cell lines. The method applied is similar to that reported by Skehan *et al.*[41] using 20 Sulfo-Rhodamine-B stain (SRB). Cells were plated in a 96-multiwell plate (104 cells per well) for 24 h before treatment with the test compound to allow attachment of the cell to the wall of the plate. Different concentrations of the compound under test (0, 1.0, 2.5, 5.0, and 10 μg ml^{-1}) were added to the cell monolayer in triplicate wells individual dose, and monolayer cells were incubated with the compounds for 48 h at 37 °C and in an atmosphere of 5% CO_2. After 48 h, cells were fixed, washed and stained with SRB stain, excess stain was washed with acetic acid and attached stain was recovered with Tris-EDTA buffer. Color intensity was measured in an ELISA reader, and the relation between the surviving fraction and drug concentration is plotted to get the survival curve of each tumor cell line after the specified compound and the IC_{50} was calculated.

Acknowledgements

The authors thank Rennes Métropole and the Institut Universitaire de France for financial support to F.M. We are also grateful to the Spanish Government (project CTQ2009-11027/BQU).

Notes and references

1 R. Huisgen, R. Grashey and J. Sauer, *The Chemistry of Alkenes*, Interscience, New York, 1964.

2 (*a*) A. Padwa, *1,3-Dipolar Cycloaddition Chemistry*, Wiley-Interscience, New York, 1984, vol. 1–2; (*b*) K. V. Gothelf and K. A. Jorgenson, *Chem. Rev.*, 1998, **98**, 863.

3 (*a*) A. Robert, J. J. Pommeret and A. Foucaud, *C. R. Acad. Sci. Paris, Ser. C*, 1970, **270**, 1739; (*b*) J. J. Pommeret and A. Foucaud, *Tetrahedron*, 1971, **27**, 2977; (*c*) A. Derdour and F. Texier, *Can. J. Chem.*, 1985, **63**, 2245; (*d*) P. Clawson, P. M. Lunn and D. A. Whiting, *J. Chem. Soc., Perkin Trans. 1*, 1990, 159; (*e*) S. G. Ruf, J. Dietz and M. Regitz, *Tetrahedron*, 2000, **56**, 6259.

4 (*a*) C. Yoakim, N. Goudreau, G. A. McGibbon, J. O'Meara, P. W. White and W. W. Ogilvie, *Helv. Chim. Acta*, 2003, **86**, 3427; (*b*) G.-W. Wang, H.-T. Yang, P. Wu, C.-B. Miao and Y. Xu, *J. Org. Chem.*, 2006, **71**, 4346.

5 (*a*) J. J. Pommeret and A. Robert, *C. R. Acad. Sci. Paris, Ser. C*, 1971, **272**, 333; (*b*) A. Robert, J. J. Pommeret, E. Marchand and A. Foucaud, *Tetrahedron*, 1973, **29**, 463; (*c*) G. Bentabed-Ababsa, A. Derdour, T. Roisnel, J. A. Sáez, P. Pérez, E. Chamorro, L. R. Domingo and F. Mongin, *J. Org. Chem.*, 2009, **74**, 2120.

6 (*a*) A. Robert, J. J. Pommeret and A. Foucaud, *Tetrahedron Lett.*, 1971, **12**, 231; (*b*) A. Robert, J. J. Pommeret and A. Foucaud, *Tetrahedron*, 1972, **28**, 2085 Concerning the $Rh_2(OAc)_4$-catalysed synthesis of 2,5-diaryl-1,3-dioxolane, see for example: (*c*) B. Jiang, X. Zhang and Z. Luo, *Org. Lett.*, 2002, **4**, 2453; (*d*) A. E. Russell, J. Brekan, L. Gronenberg and M. P. Doyle, *J. Org. Chem.*, 2004, **69**, 5269; (*e*) C.-D. Lu, Z.-Y. Chen, H. Liu, W.-H. Hu and A.-Q. Mi, *Org. Lett.*, 2004, **6**, 3071.

7 G. Bentabed-Ababsa, A. Derdour, T. Roisnel, J. A. Sáez, L. R. Domingo and F. Mongin, *Org. Biomol. Chem.*, 2008, **6**, 3144.

8 K.-R. Meier, A. Linden, G. Mlostoñ and H. Heimgartner, *Helv. Chim. Acta*, 1997, **80**, 1190.

9 M. Baudy, A. Robert and A. Foucaud, *J. Org. Chem.*, 1978, **43**, 3732.

10 J. Pornet, L. Miginiac, K. Jaworski and B. Randrianoelina, *Organometallics*, 1985, **4**, 333.

11 P. Radha Krishna, E. Raja Sekhar and F. Mongin, *Tetrahedron Lett.*, 2008, **49**, 6768.

12 W. Benchouk, S. M. Mekelleche, B. Silvi, M. J. Aurell and L. R. Domingo, *J. Phys. Org. Chem.*, 2011, **24**, 611.

13 K. B. Wiberg, *Tetrahedron*, 1968, **24**, 1083.

14 G. S. Hammond, *J. Am. Chem. Soc.*, 1955, **77**, 334.

15 (*a*) P. Geerlings, F. De Proft and W. Langenaeker, *Chem. Rev.*, 2003, **103**, 1793; (*b*) D. H. Ess, G. O. Jones and K. N. Houk, *Adv. Synth. Catal.*, 2006, **348**, 2337.

16 (*a*) L. R. Domingo, M. J. Aurell, P. Pérez and R. Contreras, *Tetrahedron*, 2002, **58**, 4417; (*b*) P. Pérez, L. R. Domingo, M. J. Aurell and R. Contreras, *Tetrahedron*, 2003, **59**, 3117.

17 (*a*) S. Berski, J. Andres, B. Silvi and L. R. Domingo, *J. Phys. Chem. A*, 2003, **107**, 6014; (*b*) V. Polo, J. Andres, S. Berski, L. R. Domingo and B. Silvi, *J. Phys. Chem. A*, 2008, **112**, 7128; (*c*) L. R. Domingo, E. Chamorro and P. Pérez, *Lett. Org. Chem.*, 2010, **7**, 432; (*d*) L. R. Domingo and J. A. Sáez, *J. Org. Chem.*, 2011, **76**, 373.

18 L. R. Domingo, M. Arno and J. Andres, *J. Org. Chem.*, 1999, **64**, 5867.

19 L. R. Domingo, M. J. Aurell, P. Pérez and J. A. Sáez, *RSC Adv.*, 2012, **2**, 1334.

20 A. W. Bauer, W. W. M. Kirby, J. C. Sherris and M. Turck, *Am. J. Clin. Pathol.*, 1966, **45**, 493.

21 See for example: M. Dolezal, J. Zitko, Z. Osicka, J. Kunes, M. Vejsova, V. Buchta, J. Dohnal, J. Jampilek and K. Kralova, *Molecules*, 2010, **15**, 8567.

22 A. Altomare, M. C. Burla, M. Camalli, G. Cascarano, C. Giacovazzo, A. Guagliardi, A. G. G. Moliterni, G. Polidori and R. Spagna, *J. Appl. Crystallogr.*, 1999, **32**, 115.

23 G. M. Sheldrick, *Acta Crystallogr., Sect. A: Found. Crystallogr.*, 2007, **A64**, 112.

24 L. J. Farrugia, *J. Appl. Crystallogr.*, 1999, **32**, 837.

25 L. J. Farrugia, *J. Appl. Crystallogr.*, 1997, **30**, 565.

26 (*a*) A. D. Becke, *J. Chem. Phys.*, 1993, **98**, 5648; (*b*) C. Lee, W. Yang and R. G. Parr, *Phys. Rev. B*, 1988, **37**, 785.

27 W. J. Hehre, L. Radom, P. v. R. Schleyer and J. A. Pople, *Ab initio Molecular Orbital Theory*, Wiley, New York, 1986.

28 (*a*) H. B. Schlegel, *J. Comput. Chem.*, 1982, **3**, 214–218; (*b*) H. B. Schlegel, in *Geometry Optimization on Potential Energy Surface*, ed. D. R. Yarkony, World Scientific Publishing, Singapore, 1994.

29 K. Fukui, *J. Phys. Chem.*, 1970, **74**, 4161.

30 (*a*) C. González and H. B. Schlegel, *J. Phys. Chem.*, 1990, **94**, 5523; (*b*) C. González and H. B. Schlegel, *J. Chem. Phys.*, 1991, **95**, 5853.

31 (*a*) J. Tomasi and M. Persico, *Chem. Rev.*, 1994, **94**, 2027; (*b*) B. Y. Simkin and I. Sheikhet, *Quantum Chemical and Statistical Theory of Solutions-A Computational Approach*, Ellis Horwood, London, 1995, p. 78.

32 (*a*) E. Cances, B. Mennucci and J. Tomasi, *J. Chem. Phys.*, 1997, **107**, 3032; (*b*) M. Cossi, V. Barone, R. Cammi and J. Tomasi, *Chem. Phys. Lett.*, 1996, **255**, 327; (*c*) V. Barone, M. Cossi and J. Tomasi, *J. Comput. Chem.*, 1998, **19**, 404.

33 (*a*) A. E. Reed, R. B. Weinstock and F. Weinhold, *J. Chem. Phys.*, 1985, **83**, 735; (*b*) A. E. Reed, L. A. Curtiss and F. Weinhold, *Chem. Rev.*, 1988, **88**, 899.

34 (*a*) A. Savin, A. D. Becke, J. Flad, R. Nesper, H. Preuss and H. G. Vonschnering, *Angew. Chem., Int. Ed. Engl.*, 1991, **30**, 409; (*b*) A. Savin, B. Silvi and F. Colonna, *Can. J. Chem.*, 1996, **74**, 1088; (*c*) A. Savin, R. Nesper, S. Wengert and T. F. Fassler, *Angew. Chem., Int. Ed. Engl.*, 1997, **36**, 1809; (*d*) B. Silvi, *J. Mol. Struct. (THEOCHEM)*, 2002, **614**, 3.

35 S. Noury, X. Krokidis, F. Fuster and B. Silvi, *Comput. Chem.*, 1999, **23**, 597.

36 M. J. Frisch, G. W. Trucks, H. B. Schlegel, G. E. Scuseria, M. A. Robb, J. R. Cheeseman, G. Scalmani, V. Barone, B. Mennucci, G. A. Petersson, H. Nakatsuji, M. Caricato, X. Li, H. P. Hratchian, A. F. Izmaylov, J. Bloino, G. Zheng, J. L. Sonnenberg, M. Hada, M. Ehara, K. Toyota, R. Fukuda, J. Hasegawa, M. Ishida, T. Nakajima, Y. Honda, O. Kitao, H. Nakai, T. Vreven, J. A. Montgomery, Jr., J. E. Peralta, F. Ogliaro, M. Bearpark, J. J. Heyd, E. Brothers, K. N. Kudin, V. N. Staroverov, R. Kobayashi, J. Normand, K. Raghavachari, A. Rendell, J. C. Burant, S. S. Iyengar, J. Tomasi, M. Cossi, N. Rega, J. M. Millam, M. Klene, J. E. Knox, J. B. Cross, V. Bakken, C. Adamo, J. Jaramillo, R. Gomperts, R. E. Stratmann, O. Yazyev, A. J. Austin, R. Cammi, C. Pomelli, J. W. Ochterski, R. L. Martin, K. Morokuma, V. G. Zakrzewski, G. A. Voth, P. Salvador, J. J. Dannenberg, S. Dapprich, A. D. Daniels, O. Farkas, J. B. Foresman, J. V. Ortiz, J. Cioslowski and D. J. Fox, *GAUSSIAN 09 (Revision A.02)*, Gaussian, Inc., Wallingford CT, 2009.

37 R. G. Parr, L. von Szentpaly and S. Liu, *J. Am. Chem. Soc.*, 1999, **121**, 1922.

38 (*a*) R. G. Parr and R. G. Pearson, *J. Am. Chem. Soc.*, 1983, **105**, 7512; (*b*) R. G. Parr and W. Yang, *Density Functional Theory of Atoms and Molecules*, Oxford University Press, New York, 1989.

39 (*a*) L. R. Domingo, E. Chamorro and P. Pérez, *J. Org. Chem.*, 2008, **73**, 4615; (*b*) L. R. Domingo and P. Pérez, *Org. Biomol. Chem.*, 2011, **9**, 7168.

40 W. Kohn and L. J. Sham, *Phys. Rev. A*, 1965, **140**, 1133.

41 P. Skehan, R. Storeng, D. Scudiero, A. Monks, J. McMahon, D. Vistica, J. T. Warren, H. Bokesch, S. Kenney and M. R. Boyd, *J. Natl. Cancer Inst.*, 1990, **82**, 1107.

